J|A|C|S
ARTICLES
Published on Web 09/26/2002

Structural Analysis of Amylose Tris(3,5-dimethylphenylcarbamate) by NMR Relevant to Its Chiral Recognition Mechanism in HPLC

Chiyo Yamamoto, Eiji Yashima,† and Yoshio Okamoto*

Contribution from the Department of Applied Chemistry, Graduate School of Engineering, Nagoya University, Chikusa-ku, Nagoya 464-8603, Japan

Received June 10, 2002

Abstract: The structural analysis of amylose tris(3,5-dimethylphenylcarbamate) (ADMPC) was performed by NMR spectroscopy using a sample with a lower degree of polymerization in order to understand the chiral recognition mechanism when it was used as a chiral stationary phase (CSP) in high-performance liquid chromatography (HPLC). ADMPC exhibited chiral discrimination for many enantiomers, including 1-(9-anthryl)-2,2,2-trifluoroethanol (**1**) and 1,1′-bi-2-naphthol (**2**) in both NMR and HPLC. A good agreement was observed between the HPLC and NMR results when chloroform was employed as the common solvent. The structure of ADMPC in solution was investigated by NMR using the 2D NOESY technique coupled with computer modeling, and a left-handed 4/3 helical structure was obtained as the most probable one. The binding geometry between ADMPC and the enantiomers of **1** was also investigated by ^{1}H NMR titration. On the basis of these results combined with molecular modeling, a rational model to explain the chiral discrimination mechanism of **1** on ADMPC was proposed.

Introduction

Phenylcarbamate derivatives of polysaccharides such as cellulose and amylose show a high chiral recognition for various enantiomers when they are used as chiral stationary phases (CSPs) for high-performance liquid chromatography (HPLC).[1] The resolving abilities of the phenylcarbamate derivatives significantly depend on the substitutions on the phenyl group, and therefore, many CSPs consisting of phenylcarbamate derivatives for HPLC have been prepared. Among them, the 3,5-dimethylphenylcarbamates of both cellulose[2] and amylose[3] show a particularly high chiral recognition for many racemates and appear to be among the most practically useful CSPs.[1b] However, their chiral recognition mechanism is still obscure, since the derivatives are soluble only in polar solvents such as pyridine and tetrahydrofuran (THF), in which one cannot detect chiral recognition by NMR spectroscopy because of the stronger interaction between the polar solvents and the phenylcarbamate derivative.[2] Moreover, the precise structure determination of the polysaccharide derivatives in the solid state and in solution is often difficult, although this is essential in order to elucidate the chiral recognition mechanism at a molecular level. We found that cellulose tris(5-fluoro-2-methylphenylcarbamate)[4] is soluble in chloroform and exhibits a high chiral recognition ability to 1,1′-bi-2-naphthol enantiomers in NMR as well as in HPLC. The binding geometry and dynamics between cellulose tris(5-fluoro-2-methylphenylcarbamate) and the enantiomers could be investigated on the basis of spin−lattice relaxation time, ^{1}H NMR titrations, and intermolecular NOEs in the presence of cellulose tris(5-fluoro-2-methylphenylcarbamate), and a rational model for the complex was able to be proposed using the structural data of the cellulose trisphenylcarbamate determined by X-ray analysis.[5] In addition, the interaction energies between the $CDCl_3$-insoluble cellulose derivatives, cellulose trisphenylcarbamate and cellulose tris(3,5-dimethylphenylcarbamate), and enantiomers have been calculated by using computational methods with molecular mechanic (MM) and molecular dynamic (MD) simulations to gain insight into the mechanism; the results of the calculations were in good agreement with the chromatographic resolution results.[6]

On the other hand, the structures of the amylose phenylcarbamate derivatives have not yet been determined by X-ray, and the amylose phenylcarbamate derivatives including ADMPC

* To whom correspondence should be addressed. E-mail: okamoto@apchem.nagoya-u.ac.jp.

† Present address: Department of Molecular Design and Engineering, Graduate School of Engineering, Nagoya University, Chikusa-ku, Nagoya 464-8603, Japan.

(1) Reviews: (a) Okamoto, Y.; Yashima, E. *Angew. Chem., Int. Ed.* **1998**, *37*, 1020−1043. (b) Yashima, E.; Yamamoto, C.; Okamoto, Y. *Synlett* **1998**, 344−360. (c) Yashima, E. *J. Chromatogr., A* **2001**, *906*, 105−125. (d) Yashima, E.; Okamoto, Y. *Bull. Chem. Soc. Jpn.* **1995**, *68*, 3289−3307. (e) Okamoto, Y.; Kaida, Y. *J. Chromatogr., A* **1994**, *666*, 403−419. (f) Dingene, J. In *A Practical Approach to Chiral Separations by Liquid Chromatography*; Subramanian, G., Ed.; VCH: New York, 1994; Chapter 6. (g) Shibata, T.; Okamoto, I.; Ishii, K. *J. Liq. Chromatogr.* **1986**, *9*, 313−340. (h) Oguni, K.; Oda, H.; Ichida, A. *J. Chromatogr., A* **1995**, *694*, 91−100.

(2) Okamoto, Y.; Kawashima, M.; Hatada, K. *J. Chromatogr.* **1986**, *363*, 173−186.

(3) Okamoto, Y.; Aburatani, R.; Fukumoto, T.; Hatada, K. *Chem. Lett.* **1987**, 1857−1860.

(4) Yashima, E.; Yamamoto, C.; Okamoto, Y. *J. Am. Chem. Soc.* **1996**, *118*, 4036−4048.

(5) Vogt, U.; Zugenmaier, P. *Ber. Bunsen-Ges. Phys. Chem.* **1985**, *89*, 1217−1224.

(6) (a) Yashima, E.; Yamada, M.; Kaida, Y.; Okamoto, Y. *J. Chromatogr., A* **1995**, *694*, 347−354. (b) Yamamoto, C.; Yashima, E.; Okamoto, Y. *Bull. Chem. Soc. Jpn.* **1999**, *72*, 1815−1825.

Chart 1. Structures of Amylose Tris(3,5-dimethylphenylcarbamate) (ADMPC) and 1-(9-Anthryl)-2,2,2-trifluoroethanol (**1**)

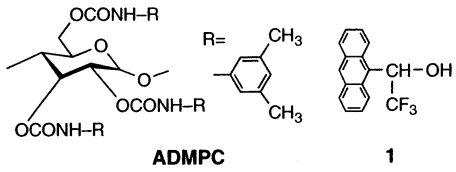

ADMPC **1**

(Chart 1) with a high degree of polymerization (DP) and amylose trisphenylcarbamate are also soluble only in polar solvents. Therefore, we could not explore the interaction between the amylose derivatives and enantiomers by means of NMR and calculations because of their poor solubility in chloroform and the lack of structural information about the amylose derivatives, respectively. However, recently, we found that low-molecular-weight (DP $\approx$ 100) ADMPC prepared by the enzymatic polymerization of α-D-glucose 1-phosphate dipotassium catalyzed by a phospholylase isolated from potato using maltopentaose as a primer[7,8] is soluble in chloroform and exhibits chiral discrimination toward many enantiomers in NMR as well as in HPLC. This prompted us to investigate the interaction between ADMPC and enantiomers in solution. To propose a rational model for the chiral recognition mechanism, the exact structure of ADMPC in solution should be determined by NMR because of the absence of X-ray data of ADMPC and its derivatives.

In this study, the structure of ADMPC was investigated by NMR using the 2D NOESY technique combined with computer modeling, and the comparison of the NMR and HPLC results in the same solvent (chloroform) was performed. The binding geometry of ADMPC−(*S*)-1-(9-anthryl)-2,2,2-trifluoroethanol (**1**) was also investigated by ^{1}H NMR titration and molecular modeling.

Results and Discussion

NOESY Studies. The recent development of 2D NMR techniques has provided a very powerful tool for the elucidation of the exact structures of biopolymers and synthetic polymers.[9] One of the promising techniques is NOESY spectroscopy, which measures the through-space interaction between nuclei.[10] For protons in polymer systems, the strength of the through-space interactions depends on the distance between them, which allows for the calculation of the interproton distances and the conformation of a polymer in solution at a molecular level. Figure 1 shows the NOESY spectrum of ADMPC; a number of NOE cross peaks were observed in the region of glucose−glucose

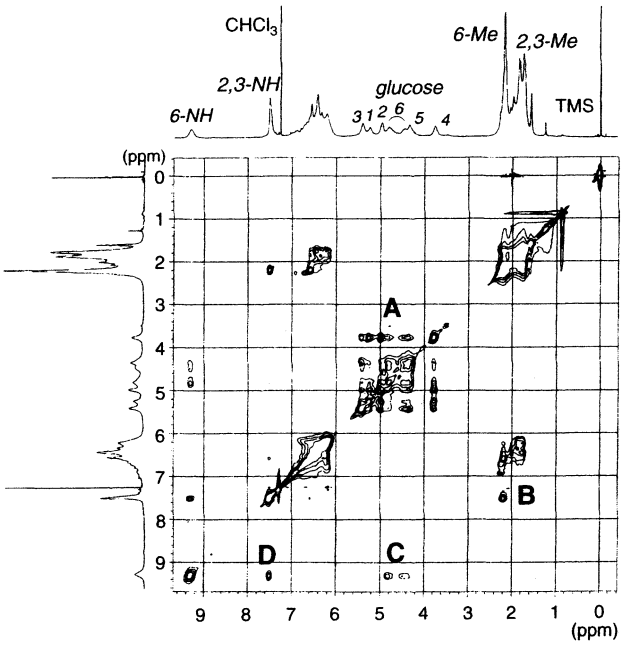

Figure 1. 500 MHz NOESY spectrum of ADMPC at a mixing time of 50 ms in $CDCl_3$ at 30 °C.

(A), NH of carbamate residues−methyl on the phenyl group (B), NH−glucose (C), and NH−NH proton resonances (D). The chemical shifts of the glucose protons (H1−H6) of ADMPC were assigned from the COSY experiment. The assignments of the methyl protons on the phenyl groups and NH protons resonances at the 2,3- or 6-position of a glucose unit were attained by comparing the NMR data of the regioselectively carbamoylated model polymers, amylose 6-(3,5-dichlorophenylcarbamate)-2,3-bis(3,5-dimethylphenylcarbamate) and amylose 2,3-bis(3,5-dichlorophenylcarbamate)-6-(3,5-dimethylphenylcarbamate).[11] The assignment of the two methyl protons at the 2- and 3-positions has not yet been attained because of the difficulty of regioselective substitution on the two hydroxyl groups at the 2- and 3-positions of a glucose.

To propose a structure for ADMPC, the interproton distances of the glucose protons must be determined, for example, H1−H4′ (the prime symbol represents a nucleus of the adjacent glucose residue), by measuring the peak volumes of the cross and diagonal peaks at different short mixing times. These distances can be related to the torsion angle about the glycoside bond defined by two dihedral angles, H1−C1−O−C4′ (ϕ) and H4′−C4′−O−C1 (ψ) (Figure 2).

The peak volumes of the cross peaks in the glucose proton resonances of ADMPC were first estimated using the 2D NOESY method acquired at different short mixing times (25−

(7) Enomoto, N.; Furukawa, S.; Ogasawara, Y.; Akano, H.; Kawamura, Y.; Yashima, E.; Okamoto, Y. *Anal. Chem.* **1996**, *68*, 2798−2804.
(8) (a) Cori, G. T.; Cori, C. F. *J. Biol. Chem*. **1940**, *135*, 733−756. (b) Pfannemüller, B.; Burchard, W. *Makromol. Chem.* **1969**, *121*, 1−17. (c) Kitamura, S.; Yunokawa, H.; Mitsuie, S.; Kuge, T. *Polym. J.* **1982**, *14*, 93−99.
(9) (a) Bax, A. In *Two-Dimensional Nuclear Magnetic Resonance in Liquids*; Delft University Press: Holland, 1984. (b) Dabrowski, J. In *Two-Dimensional NMR Spectroscopy. Application for Chemists and Biochemists*; Croasmun, W. R., Carlson, R. M. K., Eds.; VCH: New York, 1994; pp 741−783. (c) Morris, G. *Magn. Reson. Chem.* **1986**, *24*, 371−403. (d) Mirau, P. A.; Bovey, F. A. *Macromolecules* **1986**, *19*, 210−215. (e) Gippert, G. P.; Brown, L. R. *Polym. Bull*. **1984**, *11*, 585−592. (f) Scarsdale, J. N.; Prestegard, J. H.; Ando, S.; Hori, T.; Yu, R. K. *Carbohydr. Res.* **1986**, *155*, 45−56. (g) Bacon, B. E.; Cherniak, R. *Carbohydr. Res*. **1995**, *276*, 365−386. (h) Rinaldi, P. L.; Ray, D. G.; Vincent, V. E.; Keifer, P. A. *Polym. Int*. **1995**, *36*, 177−185. (i) Paramonov, N. A.; Parolis, L. A. S.; Parolis, H.; Boán, I. F.; Antón, J.; Rodríguez-Valera, F. *Carbohydr. Res*. **1998**, *309*, 89−94.
(10) (a) Mirau, P. A.; Bovey, F. A.; Tonelli, A. E.; Heffner, S. A. *Macromolecules* **1987**, *20*, 1701−1707. (b) Mirau, P. A.; Bovey, F. A. *J. Am. Chem. Soc.* **1986**, *108*, 5130−5134. (c) Kumar, A.; Wagner, G.; Ernst, R.; Wuthrich, K. *J. Am. Chem. Soc.* **1981**, *103*, 3654−3658. (d) Jansson, P.-E.; Kenne, L.; Wehler, T. *Carbohydr. Res.* **1987**, *166*, 271−282. (e) Bruch, M. D.; Bovey, F. A. *Macromolecules* **1984**, *17*, 978−981. (f) Dobson, C. M.; Olejniczak, E. T.; Poulsen, F. M.; Ratcliffe, R. G. *J. Magn. Reson*. **1982**, *48*, 97−110. (g) Macura, S.; Wuthrich, K.; Ernst, R. R. *J. Magn. Reson*. **1982**, *47*, 351−357. (h) Ellena, J.; Hutton, W. C.; Cafiso, D. S. *J. Am. Chem. Soc.* **1985**, *107*, 1530−1537. (i) Keepers, J. W.; James, L. T. *J. Magn. Reson*. **1984**, *57*, 404−426. (j) Perrin, C. L.; Gipe, R. K. *J. Am. Chem. Soc.* **1984**, *106*, 4036−4038. (k) Johnston, E. R.; Dellwo, M. J.; Hendrix, J. *J. Magn. Reson*. **1986**, *66*, 399−409. (l) Esposito, G.; Pastore, A. *J. Magn. Reson*. **1988**, *76*, 331−336.
(11) Okamoto, Y.; Aburatani, R.; Hatada, K. *Bull. Chem. Soc. Jpn.* **1990**, *63*, 955−957.

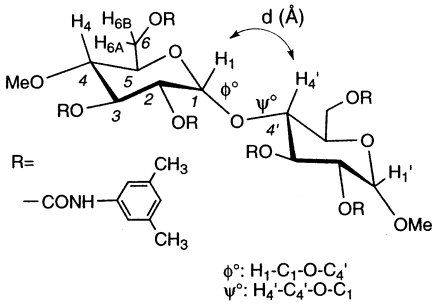

Figure 2. Dimer structure of ADMPC. Glycoside bond (H1−C1−O−C4′−H4′) is defined by two dihedral angles (ϕ, ψ).

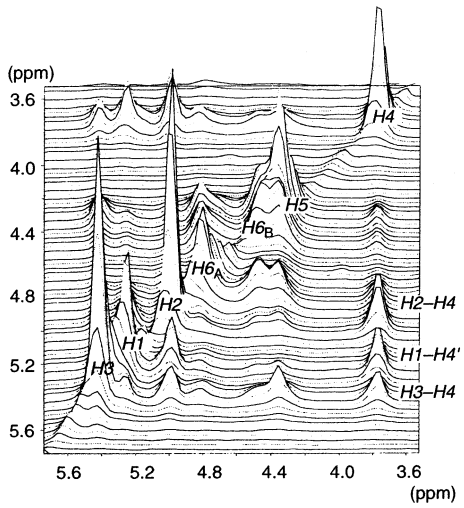

Figure 3. Stack plot of a NOESY spectrum of ADMPC at a mixing time of 50 ms in the region between glucose protons in $CDCl_3$ at 30 °C.

50 ms) according to Buchanan's method.[12] Figure 3 shows the expanded 2D NOESY spectrum in the glucose−glucose region. The diagonal elements correspond to the 1D ^{1}H NMR spectrum, and the cross peaks represent the through-space interactions between the glucose protons from which the interproton distances information can be extracted. The peak volumes of both the diagonal and cross peaks vary as a function of mixing time; the peak volumes of the diagonal peaks decay with an increase in the mixing time, while those of the cross peaks increase until they reach a maximum value after which they decrease again.

The cross peak volumes ($\mathbf{A}(\tau_m)$) as a function of the mixing time (τ_m) can be described as follows (equation 1): where $\mathbf{A}_0$ values are the peak volumes at zero mixing time obtained by extrapolating the peak volumes to zero mixing time, and **R** is the matrix (equation 2) of the relaxation rates (the diagonal ($i = j$) and off-diagonal ($i \neq j$)),[13]

$$\mathbf{A}(\tau_m) = \mathbf{A}_0 e^{-\mathbf{R}\tau_m} \tag{1}$$

$$\mathbf{R} = \begin{bmatrix} R_{ii} & \sigma_{ij} & \cdot & \cdot \\ \sigma_{ji} & R_{jj} & \cdot & \cdot \\ \cdot & \cdot & \cdot & \cdot \\ \cdot & \cdot & \cdot & \cdot \end{bmatrix} \tag{2}$$

(12) Buchanan, C. M.; Hyatt, J. A.; Lowman, D. W. *J. Am. Chem. Soc.* **1989**, *111*, 7312−7319.
(13) (a) Jeener, J.; Meier, B. H.; Bachman, P.; Ernst, R. R. *J. Chem. Phys.* **1979**, *71*, 4546−4553. (b) Macura, S.; Ernst, R. R. *Mol. Phys.* **1980**, *41*, 95−117.

Table 1. Proton−Proton Distances (Å) of Amylose[16] and Amylose Ester Derivatives[17] Estimated by X-ray Analysis

	ATV[a]	ATisoB[b]	ATA II[c]	amylose[d]
left-handed helix	5/4	4/3	9/7	6/5
H1−H4	4.10	4.10	4.09	3.97
H1−H4′	2.35	2.93	2.72	2.26
H2−H4	2.56	2.63	2.62	2.59
H3−H4	2.98	2.98	2.98	2.97
H5−H4	2.98	2.98	2.98	2.97

[a] ATV: amylose trivalerate. [b] ATisoB: amylose triisobutyrate. [c] ATA II: amylose triacetate II. [d] Potassium hydroxide amylose dodecahydrate.

The experimentally measured peak volumes ($\mathbf{A}(\tau_m)$) and the peak volumes at zero mixing time ($\mathbf{A}_0$) can be used to determine the relaxation rate matrix at each τ_m.[10g−j,14]

In the NOESY spectra, one may not observe a cross peak for protons that are separated from each other by more than 4 Å.[15] Cross peak overlapping with other peaks and those derived from both the same and adjacent glucose protons cannot be used to determine the proton distance because of the lack of accuracy, and therefore, some isolated cross peaks were selected to determine the peak volumes (in this case, H2−H4, H1−H4′, and H3−H4) and the cross relaxation rates (σ_{ij} and σ_k) were estimated. The cross relaxation rates depend on the inverse sixth power of the proton distance. Therefore, we can estimate the desired proton distance (r_{ij}) if the proton distance (r_k) is known or determined to be used as the internal reference in eq 3.

$$\frac{\sigma_{ij}}{\sigma_k} = \frac{r_{ij}^{-6}}{r_k^{-6}} \tag{3}$$

In this estimation of interproton distances, the geminal protons ($H6_A$ and $H6_B$) at C6 appear suitable as the internal reference.[12] However, in the case of ADMPC, the geminal proton peaks seriously overlap with the H5 and H2 protons, which does not allow for the accurate determination of the individual peak volumes. Therefore, we examined the other proton distances in the same glucose ring of amylose and several amylose ester derivatives which have been determined by X-ray analysis (Table 1).[16,17] Although these ester derivatives have a left-handed helical structure with a different pitch, there exist only slight differences in the proton distances H2−H4 and H3−H4. This indicates that the interproton distances in the same glucose ring seem to be independent of the structure of the amylose derivatives. Moreover, the interproton distances for H1−H4 are more than 4 Å, and therefore, the cross peak can be regarded from the H1 and H4′ protons. Using the proton distances H2−H4 and H3−H4 in the same glucose unit as the internal reference, the distance of the H1−H4′ protons was estimated to be 2.83−2.96 Å.

Structure of ADMPC. To obtain information about the glycoside bond geometry between two adjacent glucose rings, a dimer model of ADMPC shown in Figure 2 was constructed and the H1−H4′ distance and energy profiles depending on the two dihedral angles defined by ϕ and ψ were calculated; ϕ and

(14) (a) Olejniczak, E. T.; Gampe, R. T.; Fasik, S. *J. Magn. Reson.* **1986**, *67*, 28−41. (b) Massefski, W.; Bolton, P. H. *J. Magn. Reson.* **1985**, *65*, 526−530.
(15) Ernst, R. R.; Bodenhausen, G.; Wokum, A. In *Principles of Nuclear Magnetic Resonance in One and Two Dimensions*; Oxford Scientific Publications: Oxford, U.K., 1986.
(16) Sarko, A.; Biloski, A. *Carbohydr. Res.* **1980**, *79*, 11−21.
(17) Zugenmaier, P.; Steinmeier, H. *Polymer* **1986**, *27*, 1601−1608.

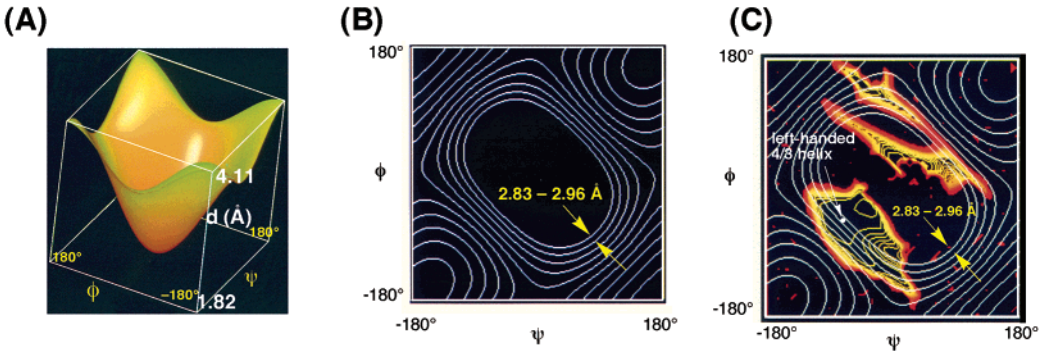

Figure 4. Three-dimensional distance (A) and energy profiles (C) of the dimer model of ADMPC. The contour map (B) is extracted from part A, and contours are drawn by 0.13 Å intervals. The total energy contour map is superimposed with the distance contour map (C).

ψ were individually rotated at 6° intervals, and the distance of the H1−H4′ protons and the potential energy were estimated in order to plot the three-dimensional distance (Figure 4A) and energy profiles (Figure 4C). Figure 4B shows the contour map extracted from Figure 4A. The contours are drawn in 0.13-Å intervals, and the total energy map was superimposed in Figure 4B (Figure 4C). There are numerous possible dihedral angles which satisfy the estimated H1−H4′ distance (2.83−2.96 Å). The total energy contour map estimated from the dimer model of ADMPC in Figure 4C shows the areas with high total energies in black, and the total energies decrease when the color gradually changes from red to yellow. The energy profile combined with the distance profile indicates the combination of (ϕ, ψ) satisfying the distance of H1−H4′ (2.83−2.96 Å), and the lowest total energy of the dimer is (−68.5°, −42.0°) indicated by a white arrow. This dihedral angle leads to the left-handed 4/3 helical structure for ADMPC. There is one more dihedral angle around (+68°, +42°) satisfying the distance and the low total energy. However, this dihedral angle leads to the right-handed helical structure for ADMPC, and therefore, it was discarded.

The polymer model of ADMPC was then constructed using the obtained dihedral angles and optimized under three-dimensional periodic boundary conditions according to the reported method.[4,6,18] The full structure of ADMPC is shown in Figures 5A and B, while the main chain is shown in Figures 5C and D for clarity. The optimized structure of ADMPC has a similar left-handed 4/3 helix to that of amylose triisobutyrate (ATisoB),[17] and the glucose residues are regularly arranged along the helical axis. A chiral helical groove with polar carbamate groups exists along the main chain. The polar carbamate groups are preferably located inside, and the hydrophobic aromatic groups are placed outside the polymer chain so that polar enantiomers may predominantly interact with the carbamate residues in the groove through hydrogen bond formation. Recently, Wenslow amd Wang examined the structure analysis of ADMPC by solid-state NMR.[19] They pointed out that ADMPC has a helical structure with less than six folds.

Chiral Recognition in NMR and HPLC. As described above, ADMPC of DP < 100 is soluble in chloroform, and this enabled us to investigate the interactions between ADMPC and a racemate in chloroform by NMR spectroscopy. On the other hand, we developed the chemically bonded-type CSP with

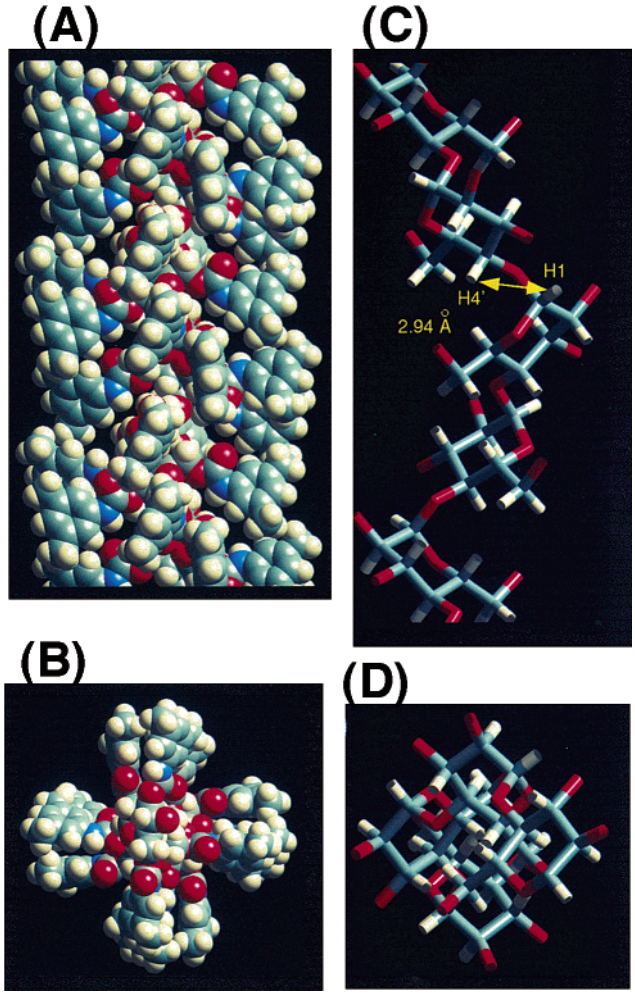

Figure 5. Optimized structure (A and B) and the main chain (C and D) of ADMPC. The viewpoints are along the chain axis (A and C) and perpendicular to the chain axis (B and D).

ADMPC which allows us to use chloroform as the eluent in HPLC.[7] Therefore, we can directly compare the results in HPLC with those in NMR using the same chloroform solvent. Table 2 summarizes the results of the chiral discrimination for some racemates in ^{1}H and ^{19}F NMR using ADMPC as a chiral selector and the data on the chromatographic enantioseparation on the ADMPC-based CSP using hexane/2-propanol (9/1, v/v) and dry chloroform as the eluents. When the enantiomers are eluted at retention times t_1 and t_2, the capacity factors (k_1' and k_2') and separation factors (α) can be evaluated as $(t_1 - t_0)/t_0$, $(t_2 - t_0)/t_0$, and $\alpha = k_2'/k_1'$, respectively. The dead time (t_0) has been

(18) Yashima, E.; Noguchi, J.; Okamoto, Y. *Macromolecules* **1995**, *28*, 8368−8374.
(19) Wenslow, R. M., Jr.; Wang, T. *Anal. Chem.* **2001**, *73*, 4190−4195.

Table 2. Chiral Discrimination for **1**−**9** by ADMPC in HPLC and NMR

No.	structure	HPLC [a]		NMR
		α (Hex/IPA)[b]	α ($CHCl_3$)[c]	ΔΔδ (ppm)[d]
1	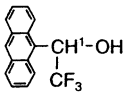	k_1'=1.81 α=1.39 (–)	k_1'=1.59 α=1.36 (+)	^{1}H) OH: –0.032 (+) H^1: +0.010 (–) ^{19}F) N.S[e]
2	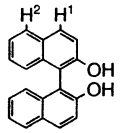	k_1'=8.21 α=1.09 (–)	k_1'=0.74 α=1.57 (+)	^{1}H) OH: –0.134 (+) H^1: +0.009 (–) H^2: +0.008 (–)
3	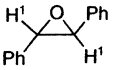	k_1'=0.42 α=3.04 (–)	k_1'=0.08 α=2.44 (–)	^{1}H) H^1: –0.010 (–)
4	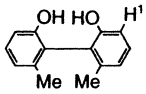	k_1'=2.46 α=2.11 (+)	k_1'=1.01 α=1.72 (+)	^{1}H) OH: –0.198 (+) H^1: +0.010 (–)
5	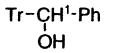	k_1'=2.65 α=1.98 (–)	k_1'=0.21 α=1.61 (–)	^{1}H) H^1: –0.013
6	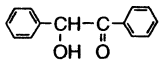	k_1'=3.14 α=1.21 (+)	k_1'=0.32 α=1.00	^{1}H) N.S
7	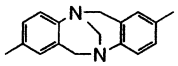	k_1'=0.53 α=1.58 (–)	k_1'=0.03 α=1.00 (–)	^{1}H) N.S
8	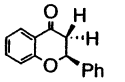	k_1'=0.93 α=1.05 (–)	k_1'=0.11 α=1.00	^{1}H) N.S
9		k_1'=0.09 α=~1 (+)	k_1'=0.10 α=~1 (+)	^{1}H) N.S

[a] Flow rate, 0.5 mL min^{-1}. The sign in parentheses represents the optical rotation of the second eluted enantiomer. [b] CSP, coated type; eluent, hexane/2-propanol (90/10). [c] CSP, chemically bonded type; eluent, dry $CHCl_3$. [d] $\Delta\Delta\delta$ (= $|\Delta\delta S - \Delta\delta R|$) indicates the difference in the chemical shift between enantiomers. $\Delta\delta$ (= $\delta f - \delta$) indicates the induced shift of the enantiomers in the presence of ADMPC. δ and δf are the chemical shifts of a particular proton of a racemate in the presence and absence of ADMPC, respectively. Negative values indicate downfield shift. The sign in parentheses represents the optical rotation of the more shifted enantiomer. [e] Not separated.

estimated using 1,3,5-tri-*tert*-butylbenzene as a nonretained compound.[20]

The capacity factors for most racemates using chloroform as the eluent were smaller than those using hexane/2-propanol as the eluent, and the racemates **6**−**9** were not resolved with chloroform; the elution order of the enantiomers of **1** and **2** was reversed in the two eluent systems. Figure 6 shows the resolution of **1** on the ADMPC CSP with hexane/2-propanol and chloroform as the eluents. The HPLC results using chloroform as the eluent agreed with the NMR results; the OH proton of the (*S*)-(+)-**1** was more significantly shifted downfield than that of the corresponding (*R*)-(−)-**1** in NMR (Figure 7), indicating that (*S*)-**1** interacts more strongly with ADMPC than (*R*)-**1**. The downfield shift of the OH proton may be ascribed to hydrogen bond formation.[21,22]

Interaction of ADMPC and (*S*)-1. The ^{1}H NMR titrations of ADMPC with (*S*)- and (*R*)-**1** were performed in order to obtain information with respect to the binding sites of ADMPC

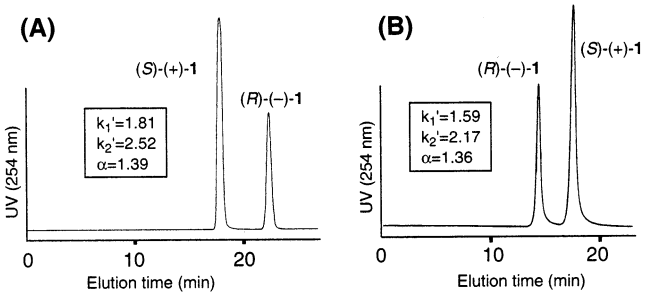

Figure 6. Chromatograms of the enantioseparation of **1** on coated-type ADMPC with hexane/2-propanol (90/10) as the eluent (A) and chemically bonded-type ADMPC with $CHCl_3$ as the eluent (B) at 25 °C. Column, 25 cm × 0.46 cm (i.d.); flow rate, 0.5 mL min^{-1}. The (*S*)-/(*R*)-**1** mixed ratio is 2/1.

in the complexation. Figure 8 shows the ^{1}H NMR spectra of the glucose proton (H1−H6) region of ADMPC in the absence and the presence of (*S*)-**1**. The H1, H2, and H4 proton resonances of a glucose unit of ADMPC were significantly affected by the addition of (*S*)-**1** and shifted upfield, whereas the other glucose proton resonances only slightly moved. The significant upfield shifts of the three proton resonances indicate that an anthryl ring of (*S*)-**1** may be closely located above the H1, H2, and H4 protons on the same side of the glucose ring

(20) Koller, H.; Rimböck, K.-H.; Mannschreck, A. *J. Chromatogr.* **1983**, *282*, 89−94.
(21) Feibush, B.; Figueroa, A.; Charles, R.; Onan, K. D.; Feibush, P.; Karger, B. L. *J. Am. Chem. Soc.* **1986**, *108*, 3310−3318.
(22) (a) Dobashi, Y.; Dobashi, A.; Ochiai, H.; Hara, S. *J. Am. Chem. Soc.* **1990**, *112*, 6121−6123. (b) Nishiyama, H.; Tajima, T.; Takayama, M.; Itoh, K. *Tetrahedron: Asymmetry* **1993**, *4*, 1461−1464.

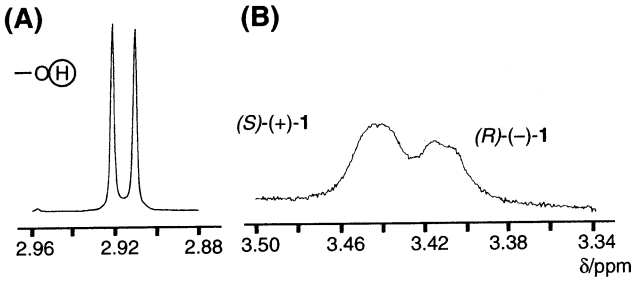

Figure 7. ^{1}H NMR spectra of the OH proton of **1** (20.1 mM) in the absence (A) and presence (B) of ADMPC (36.8 mM glucose units) in $CDCl_3$ at 23 °C.

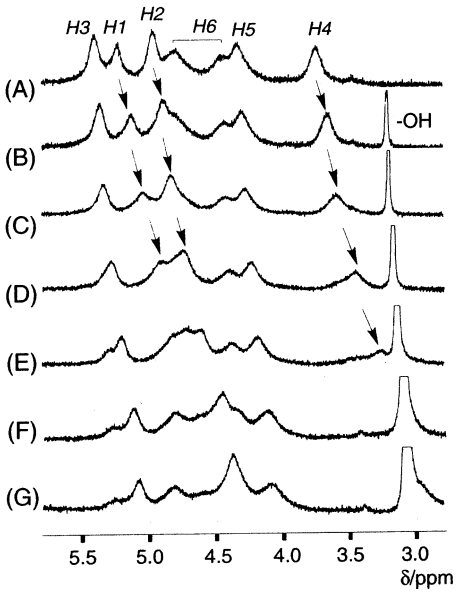

Figure 8. Changes of glucose proton resonances (H1−H6) of ADMPC in the absence (A) and presence of (*S*)-(+)-**1** (1.2 (B), 2.5 (C), 5.0 (D), 10 (E), 20 (F), and 30 mg (G)) in $CDCl_3$ at 23 °C.

so that it can significantly affect its ring current. The movement of the glucose protons' chemical shifts in the presence of (*R*)-**1** was relatively small.

The HPLC and NMR experiments demonstrated that (*S*)-**1** is above the H1, H2, and H4 protons of the glucose in a chiral groove of ADMPC through intermolecular hydrogen bonding between the OH proton of the (*S*)-**1** and probably the carbonyl oxygen of ADMPC. Although the 2D NOESY spectra of the ADMPC−(*S*)-**1** complex were measured under various conditions, clear intermolecular NOEs for the complex have not yet been observed. Therefore, a precise model for the complex cannot be proposed. However, on the basis of the HPLC and NMR titration data, a model structure for the ADMPC−(*S*)-**1** complex can be proposed. The energy-minimized (*S*)-**1** was manually placed in the groove of the main chain of ADMPC so that the ^{1}H NMR titration results as well as the intermolecular hydrogen bonds were visually satisfied. The complex was energy minimized further to relieve the unfavorable van der Waals contacts. Figure 9 shows the lowest energy structure of the ADMPC−(*S*)-**1** complex. The OH proton of (*S*)-**1** forms hydrogen bonding with the carbonyl oxygen of the carbamate group at the 2-position. The distance between the hydrogen and oxygen is 1.968 Å, which is short enough for hydrogen bonding. Moreover, the anthryl ring is favorably positioned above the H1, H2, and H4 protons, and the interaction model explains

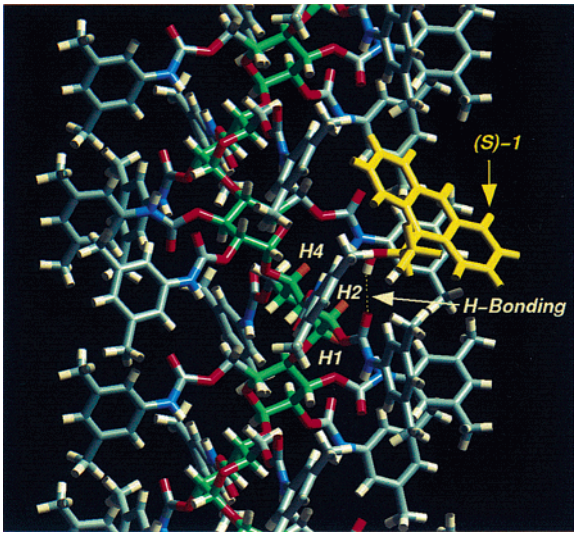

Figure 9. Computer-generated depiction of the complex of ADMPC−(*S*)-**1**. The glucose carbon atoms and the H1, H2, and H4 protons of the glucose residue of ADMPC are shown in green and orange, respectively. The dashed line corresponds to hydrogen bond.

the upfield shift of the H1, H2, and H4 protons of the glucose residue in the presence of (*S*)-**1**.

Conclusions. Low-molecular-weight ADMPC is soluble in chloroform, and exhibited chiral discrimination for many enantiomers in NMR as well as in HPLC. On the basis of the NOESY spectroscopic studies coupled with computer modeling, a left-handed 4/3 helical structure was obtained as the most probable one for ADMPC. Moreover, by using the same solvent (chloroform) in NMR and HPLC, a good agreement was observed in the chiral recognition results. These results, particularly on the structure of ADMPC, should provide useful information both for understanding the chiral discrimination mechanism on this popular CSP and for designing much better CSPs.

Experimental Section

Materials. Amylose (degree of polymerization (DP) ≈ 60 (AS-10) and DP ≈ 100 (AS-16)) and 3,5-dimethylphenyl isocyanate were kindly supplied from Nakano Vinegar (Handa, Japan) and Daicel (Osaka, Japan), respectively. (3-Aminopropyl)triethoxysilane was of guaranteed reagent grade from Tokyo Kasei. Porous spherical silica gel (Daiso gel SP-1000) with a mean particle size of 7 μm and a mean pore diameter of 100 nm was kindly supplied from Daiso Chemical. All solvents used in the preparation of the CSPs were analytically reagent grade, carefully dried, and distilled before use. Chloroform used in the chromatographic experiments was distilled in the presence of CaH_2 after removing ethanol as the stabilizer by washing with water. All other solvents were HPLC grade. $CDCl_3$ (99.8 atom %D) was purchased from Aldrich and was dried over molecular sieves 4A (Nacalai). 2,2′-Dihydroxy-6,6′-dimethylbiphenyl (**4**) was a gift from Dr. Kanoh of Kanazawa University. The other racemates (**1**−**3**, **5**−**9**) (Table 2) were commercially available or were prepared by the usual method.[23]

Synthesis of Amylose Tris(3,5-dimethylphenylcarbamate) (ADMPC). Amylose tris(3,5-dimethylphenylcarbamate) (ADMPC) was prepared according to a previously described procedure by the reaction of amylose with a large excess of 3,5-dimethylphenyl isocyanate in dry pyridine (20 mL) at ~80 °C for 24 h.[3] The obtained phenylcarbamoylated amylose derivative was isolated as a methanol-insoluble fraction and dried. After the amylose derivative was dissolved in

(23) Kaida, Y.; Okamoto, Y. *Bull. Chem. Soc. Jpn.* **1992**, *65*, 2286−2289.

chloroform, the insoluble parts were removed by filtration. The soluble parts were reprecipitated in methanol, centrifuged, and dried in vacuo at 60 °C for 2 h. The ^{1}H NMR data showed that the hydroxy groups of amylose were almost quantitatively converted into the carbamate moieties. IR (KBr) (cm^{-1}) 3381, 3324 (ν_{NH}), 1735 ($\nu_{C=O}$); ^{1}H NMR ($CDCl_3$, 20 °C, TMS) δ 1.73, 1.84, 2.18 (s, CH_3, 9H), 3.75, 4.34, 4.46, 4.82, 4.96, 5.23, 5.41 (br, glucose protons, 7H), 6.0−7.1 (br, aromatic, 9H), 7.52, 9.33 (br, NH, 3H).

Instruments. Chromatographic experiments were performed on a Jasco PU-980 chromatograph equipped with UV (Jasco 875-UV) and polarimetric (Jasco OR-990, Hg without filter) detectors. The enantioseparations were performed using two different types of CSPs; one is Chiralpak AD (Daicel), and the other is the chemically bonded-type AD[7] using hexane/2-propanol (9/1, v/v) and dry chloroform as the eluent, respectively. The latter CSP was prepared by the enzymatic polymerization of α-D-glucose 1-phosphate dipotassium catalyzed by potato phosphorylase using the primer derived from maltopentaose. A racemate solution (3 mg mL^{-1}) was injected into the chromatographic system (0.5−10 μL) using a Rheodyne Model 7125 injector. One dimensional ^{1}H and ^{19}F NMR spectra were recorded on a Varian Gemini 2000 spectrometer operating at 400 MHz for ^{1}H and 376 MHz for ^{19}F. The 2D NOESY spectra were obtained on a Varian INOVA 500 spectrometer. All NMR spectra were measured in $CDCl_3$. Chemical shifts were reported in parts per million (ppm) using tetramethylsilane (TMS, 0 ppm) and α,α,α-trifluorotoluene (−64.0 ppm) as the internal standard for the ^{1}H and ^{19}F NMR spectra, respectively.

^{1}H NMR Titration. The ^{1}H NMR titration experiments were performed in order to obtain information with respect to the binding sites of ADMPC in the complexation. The concentration of ADMPC was maintained at a constant value in the presence of the increasing concentrations of (*S*)- or (*R*)-**1**. A 18.4 mM ADMPC solution in $CDCl_3$ was prepared in a 5-mm NMR tube as the original sample. To this was directly added (*S*)- or (*R*)-**1** (1.2, 1.3, 2.5, 5.0, 10, and 10 mg, respectively), and the NMR spectra were taken for each addition.

2D NMR. The NOESY experiments were recorded in the phase sensitive mode at 30 °C without degassing. The NOESY spectra for ADMPC were collected into 1024 complex points for 256 t_1 increments with a spectral width of 6667 Hz at mixing times of 25−50 ms. The data matrix was zero filled to 1024, apodized with a Gaussian function, and then Fourier transformed in both dimensions. Cross peak volumes were obtained as the sum of the data by projecting 2D data onto the axis parallel to the screen axis with a summing algorithm.[24]

Molecular Modeling. The molecular modeling and molecular mechanic calculations were performed using the Dreiding force field (version 2.21)[25] as implemented in CERIUS^2 software (version 3.5, Molecular Simulations Inc., Burlington, MA)[26] and pcff force field[27] available with the Discover software (version 4.0.0, MSI)[28] running on an Indigo^2-Extreme or an Indigo^2-Impact work station (Silicon Graphics). The charges on the atoms of ADMPC and **1** were calculated using QEq[29] in CERIUS^2, and the total charges of the molecules were zero.

The initial structure of ADMPC was constructed using the structure of amylose triisobutyrate (ATisoB) postulated on the basis of an X-ray analysis.[17] First, a repeating unit of ADMPC was obtained by replacement of the isobutyrate with 3,5-dimethylphenylcarbamate at the 2-, 3-, and 6-positions and CH_3O at the 1- and 4-positions. The side chains at the 2-, 3-, and 6-positions of the repeating unit were then stabilized using the Conformational Search in CERIUS^2. The monomeric unit of ADMPC was allowed to construct a dimer, and the two dihedral angles defined by H1−C1−O−C4′ (ϕ) and H4′−C4′−O−C1 (ψ) were fixed at 0° as the initial structure for the calculation. Calculations of the dimer were then performed using the Phi-Psi-Map program[28] in Discover (Figure 4). Using a pair of dihedral angles (ϕ (−68.5) and ψ (−42.0)) determined by NMR and the above calculations, a 4-mer with a left-handed four fold (4/3) helix was constructed by Polymer Builder in CERIUS^2. The 4-mer was placed into a simulation cell ($x = 40$ Å, $y = 40$ Å, and $z = 15.613$ Å) under three-dimensional periodic boundary conditions by Crystal Builder in CERIUS^2. The unit cell volume was expanded in the directions perpendicular to the polymer axis (z) to avoid interactions between the periodic polymer and neighboring ones in other cells. The energy minimization was then accomplished by Conjugate Gradient 200 (CG 200) and then by Fretcher Powell (FP) until the root-mean-square (rms) value became less than 0.01 kcal mol^{-1} $Å^{-1}$.

The initial coordinates of (*S*)- and (*R*)-**1** were taken from the crystal structure data of (*RS*)-**1**[30] in the Cambridge Structural Database 2D Graphics Search System.[31] The initial structure was further energy-minimized by CG200 and FP using the Dreiding force field. The optimized (*S*)-**1** was manually placed into the interaction site of ADMPC so that the titration results in the NMR as well as intermolecular hydrogen bonds were visually satisfied. The complex was energy minimized further by CG200 and FP to relieve any unfavorable van der Waals contacts, while the geometry of ADMPC was fixed.

Acknowledgment. We thank Miss Mayuko Saito for her experimental support. We also acknowledge Dr. Shigeyoshi Kanoh (Kanazawa University) for providing **4**. This work was partially supported by Grant-in-Aids for Scientific Research on Priority Areas No. 10208103 and No. 10208206 from the Ministry of Education, Science, Sports, and Culture, Japan, and the Venture Business Laboratory Project "Advanced Nano-process Technologies" at Nagoya University.

JA020828G

(24) *VNMR 5.3 Command and Parameter Reference*; Varian.
(25) Mayo, S. L.; Olafson, B. D.; Goddard, W. A., III. *J. Phys. Chem.* **1990**, *94*, 8897−8909.
(26) *Cerius2 User's Reference Release 3.0*; Molecular Simulations Inc.: Burlington, MA.
(27) (a) Sun, H. *J. Comput. Chem.* **1994**, *15*, 752−768. (b) Sun, H. *Macromolecules* **1995**, *28*, 701−712. (c) Sun, H.; Mumby, S. J.; Maple, J. R.; Hagler, A. T. *J. Am. Chem. Soc.* **1994**, *116*, 2978−2987.
(28) *Discover 96.0/4.00 User Guide*; Molecular Simulations Inc.: Burlington, MA, 1996.
(29) Rappé A. K.; Goddard, W. A. III. *J. Phys. Chem.* **1991**, *95*, 3358−3363.
(30) Rzepa, H. S.; Webb, M. L.; Slawin, A. M. Z.; Williams, D. J. *J. Chem. Soc., Chem. Commun.* **1991**, 765−768.
(31) Allen, F. H.; Kennard, O. *Chem. Des. Autom. News* **1993**, *8*, 31.